EFFECT OF PARTICLE SIZE ON THE MECHANICAL PROPERTIES OF PERIWINKLE SHELL REINFORCED POLYESTER COMPOSITE (PRPC)

Onyechi, P.C.1, Asiegbu, K.O.1, Igwegbe, C.A.2, Nwosu, M.C.1
1 Department of Industrial and Production Engineering, Nnamdi Azikiwe University, Awka, Nigeria.
2 Department of Chemical Engineering, Nnamdi Azikiwe University, Awka, Nigeria.

ABSTRACT: The effects of particle size of periwinkle shells (PWS) on the mechanical properties of particulate reinforced polyester composite (PRPC) was investigated. Particle sizes considered were 400µm, 600µm, 766µm, 1180µm and 1760µm. Five replicated samples of each particle sizes were considered for volume fraction of 10%, 20%, 30%, 40% and 50%. 100 samples were produced and 25 of these samples were subjected to each mechanical test which include; tensile, flexural, hardness, and impact test. The average test results were used for graphical analysis with Minitab 15 software (developed in 2007). The maximum tensile strength of 24.3MPa was obtained from the composite made of 400µm particle size at 30% volume content. The maximum flexural strength of 47.4MPa was also obtained from the composite made of 400µm particle size at 30% volume content. Additionally, the composite made of 400µm particle size at 50% volume content gave the maximum hardness number (BHN) of 249. The composite made up of 1760µm particle size at 50% volume content yielded the maximum impact strength of 23.2Jm-2. It is concluded that decrease in particle sizes increases the tensile strength and flexural strength, but causes a scattered diagram in hardness strength. In impact test, the strength increases with increase in particle size. For the filler content, the tensile and the flexural strength rises highest at 30% content where it then decreases sharply, but in hardness and impact test, increase in filler content increases the BHN and impact strength.

Keywords: Composite, Filler content, Flexural, Hardness, Particle size, Periwinkle shells, Strength, Tensile.

1. INTRODUCTION

Over the last three decades, composite materials, plastics and ceramics have been the dominant emerging materials. In developing countries, harvest season are often accompanied with residues that are of environmental menace and in some cases hazardous. Many of these materials could be utilized in developing composite material as fillers. Research is proceeding to develop composites using various recycled wastes, [1,2] especially in developing composites using most environmentally friendly agro-wastes as reinforcing fillers and thermosetting polymers as matrixes. Recent investigations of polymer-based composite materials have opened new routes for polymer formulations and have allowed the manufacture of new products with optimal properties for special applications [3]. In most cases, these composites improve the product design and reduce the material and energy consumption. Today, the growing environmental awareness throughout the world has triggered a paradigm shift from synthetic fibers and their composites towards composites made from natural reinforcing constituents (natural fibers and natural particulate fillers) which are more environmentally friendly ([4, 5, 6]. In the light of this, researchers have focused their attention on composites composed of natural or synthetic resins,[7,8] reinforced with mineral particulate fillers and manufacturing of high-performance engineering materials from these renewable resources has also been pursued by researchers since renewable raw materials are environmentally sound and do not cause health problems [9]. Fillers having cellulose, hemi cellulose and lignin are being investigated for the suitability of replacing

synthetic fibers [10]. The use of these natural fillers has been due to its economic advantage during processing, high specific strength, relatively low density and biodegrability, thereby reducing environmental pollution [11,12]. Commonly used particulate fillers include; talc, calcium carbonate, kaoline, silica and carbon black. Some of these materials are not readily available, hence the need to source for other potentially suitable reinforcing constituents for polymer matrices. Harvest season are often accompanied with residues that are of environmental menace and in some cases hazardous [3]. Periwinkle shells (PWS) is one of these wastes but recently has been of some use in concrete mixing [13], and also in some locality its use is applied in road maintenance.

It is an external exoskeleton which protects the periwinkles from their predators and mechanical damage. These snails called periwinkle are found in the lagoons and mudflats of the Niger Delta between Calabar in the East and Badagry in the West of Nigeria, the people in this area consume the edible part as sea food and dispose the shell as a waste. Sample picture of these PWS is shown on figure 1.

Figure 1: Periwinkle shells

Few of these shells are utilize as coarse aggregate in concrete in areas where there are neither stones nor granite for purposes such as paving of water logged areas e.t.c., but a large amount of these shells are still disposed off as waste and with disposal already constituting a problem in areas where they cannot find any use for it, and large deposits have accumulated in many places over the years [13].

It was indicated that there are about 40.3 tonnes of periwinkle per year being harvested from 35 mangrove communities of Delta and Rivers states of Nigeria [14]. A survey, by the researchers, of some riverside communities of Itu, Oron, Issiet, Okobo, Ikot Offiong, and Uta-ewea in Akwa Ibom state showed abundance of periwinkle in these communities. Massive periwinkle harvesting is also reported from some communities in Bayelsa, Cross River and Edo states of Nigeria [15, 16]. According to Aku et al. [17], the periwinkle shell particle exhibited a density of 1.24g/cm^3. Structurally, the periwinkle shell has several layers and is typically made of an organic matrix (conchiolin) which is bonded with calcium carbonate precipitates. These calcium

carbonate-filled organic matrix shells are impervious to water and this property makes it possible for periwinkle shells and their derivatives to have very wide applications [18].

Related Work

With the growing global energy crisis and ecological risks, there is ongoing research on natural fillers reinforced polymer composites and their application in design of equipment subjected to impact loading. In most of this research polyester resin serves as the matrix. Though epoxy may have been a better properties but cost advantage of polyester plays a big role in its selection.

Davallo et al. [19], studied the mechanical behavior of unsaturated polyester resin used for the composite materials and determined various important parameters, such as tensile, single edge-notch tensile fracture toughness, flexural properties and fracture energy. Periwinkle shells which are calcium carbonate-filled organic matrix shells are impervious to water and this property makes it possible for periwinkle shells and their derivatives to have very wide applications.

Aku et al. [17], conducted an XRF analysis on these PWS and confirmed that SiO_2, CaO, MgO, Cr_2O_3, and Fe_2O_3 were found to be major constituents of the periwinkle ash. Silicon dioxide, iron oxide, Cr_2O_3 and CaO are known to be among the hardest substances. Some other oxides like K_2O, Na_2O, and MnO were also found to be present in traces. The presence of hard elements like SiO_2, CaO, Cr_2O_3, and Fe_2O_3 suggested that, the periwinkle shell particles can be used as reinforcing material.

Olutoge et al. [13], studied the suitability of periwinkle shell ash as partial replacement for ordinary Portland cement in concrete, analyzed the chemical content of periwinkle shell ash and the following constituents was gotten with their weight percentage above; ZnO, CuO, Fe_2O_3, MnO_2, MgO, SiO_2, Al_2O_3, K_2O, CaO, Na_2O.

Generally, research has been made on effects of fillers on the mechanical properties of polymer. Fu et al. [20] studied that the effects of particle size, particle-matrix adhesion and particle loading on composite stiffness, strength and toughness of a range of particulate composites both micro- and nano-fillers with small aspect ratios of unity. It was shown that composite strength and toughness are strongly affected by all these three factors, especially particle-matrix adhesion. This is expected because strength depends on effective stress transfer between filler and matrix, and toughness and brittleness is controlled by adhesion. Various trends of the effect of particle loading on composite strength and toughness have been observed due to the interplay between these three factors, which cannot always be separated. However, composite stiffness depends significantly on particle loading, not particle-matrix adhesion, since the fillers have much larger modulus than the matrix.

Studies were made by Ofem and Umar [11] on effect of filler content on the mechanical properties of periwinkle shell reinforced CNSL (cashew nut shell liquid) resin composites with particle sizes (400, 600, 800μm) and filler loading (10, 20, 30, and 40%) and reported that 30% Filler content gave the best properties, while the highest tensile and flexural strengths were recorded at 30% filler content and 400μm particle sizes, the highest tensile modulus and impact strength were recorded at 800μm particle sizes but 30% and 40% filler content respectively. At

40% filler content the properties tends to decrease indicating that the optimum properties can be achieved at 30% filler content.

According to Nwanonenyi et al [21], the effects of particle sizes, filler contents and compatibilization on the properties of linear low density polyethylene filled periwinkle shell powder practically showed that preparation of thermoplastic composite using linear low density and periwinkle shell powder is possible. The tensile strength, tensile modulus, flexural strength, impact strength, hardness, and specific gravity of the linear low density polyethylene composite were found to increase with increase in filler and compatibilizer contents respectively, and decrease in filler particle size. The periwinkle shell fillers can serve as alternative to conventional mineral fillers like talc, asbestos, silica, mica and among others in plastic composite due to the growing global environmental concern and, the high rate of depletion of petroleum and mineral resources, as well as new environmental regulations demanding the search for the composite materials that are compatible with the environment.

Ofem et al [11], later investigated the mechanical properties of the hybrid composite made of periwinkle shells (PWS) and rice husk (RH) as reinforcing fillers using cashew nut shell liquid (CNSL) resin composite as the matrix. With PWS particle sizes (400, 600, 800μm) and filler loading(10, 20, 30%), the results shows that the highest tensile and flexural strengths were obtained at 30% filler content and 400μm particle sizes, and the highest tensile modulus and impact strength were obtained at 800μm and 400μm particle sizes, respectively, for the same percentage of filler content. The flexural strength from the result converges at 30% filler content. This can however, be concluded that the optimum properties can be achieved at 30% filler content.

Njoku et al. [22], studied the effects of variation of particle size and weight fraction on the tensile strength and modulus of Periwinkle reinforced composite, and reported that:

1. Periwinkle particle size within the range of particle sizes (400 - 1000μm) studied has negligible effect on the Young's modulus of Periwinkle reinforced composite.
2. The tensile strength of Periwinkle reinforced composite increases with decreasing particle size.
3. Both tensile strength and Young's modulus of the composite material increase with increasing weight fraction of periwinkle particles in the composite laminate.

Njoku et al, [22] also showed the relationship between weight fraction and the volume fraction. .

Volume fraction

$$\upsilon_f = V_f / V_c \ , \ \upsilon_m = V_m / V_c \qquad (1)$$

Where V is volume of constituents and subscripts p, c and m refer to the particle, composite and matrix, respectively.

Similarly,

$$\omega_f = W_f / W_c , \quad \omega_m = W_m / W_c \tag{2}$$

ω_p & ω_m, are weight fractions of particle and matrix respectively and W is the weight of constituent. A relationship between the weight fraction and volume fraction can be established by introducing the density ρ of the composite and its constituents. Essentially,

$$\rho_c = \rho_f \upsilon_f + \rho_m \upsilon_m \tag{3}$$

Recalling that

$$\omega_f = W_f / W_c = \rho_f V_f / \rho_c V_c = \frac{\rho_f}{\rho_c} \upsilon_f \tag{4}$$

similarly;

$$\omega_m = W_m / W_c = \rho_m V_m / \rho_c V_c = \frac{\rho_m}{\rho_c} \upsilon_m \tag{5}$$

At any composite strain ε_c prior to fracture, the stresses in the matrix (σ_m) and particle (σ_{fp}) can be obtained from:

$$\sigma_{fp} = E_{fp} \varepsilon_c \quad \text{and} \quad \sigma_m = E_m \varepsilon_c \tag{6}$$

Where E_m and E_f are the Youngs moduli of matrix and particle respectively. The composite stress (σ_c) is given by:

$$\sigma_c = \sigma_{fp} \upsilon_{fp} + \sigma_m (1 - \upsilon_{fp}) \tag{7}$$

and the axial Youngs Modulus of the components obtained from equation below:

$$E_c = E_{fp} \upsilon_{fp} + E_m (1 - \upsilon_{fp}) \tag{8}$$

Design of Mould

In the design of the mould used in this experiment, the internal volume of the mould is considered. This internal volume of the mould is approximately equals to the volume of the composite in the mould. This implies that;

$$V_i \approx V_c \tag{9}$$

The rule of mixtures shows that the volume of composite equals the volume of matrix and the volume of PWS fillers;

$$V_i \approx V_c = V_f + V_m \quad (10)$$

If PWS contains 10% of the composite, then the matrix (polyester) will contain approximately 90% of the composite.

For a portion of PWS measured to be 36cm^3 considered for 10% of the composite, applying equation (3.10);

$$V_m = \left(\frac{1-0.1}{0.1}\right)36$$

$$V_m = 9(36) = 324cm^3$$

From equation (3.12)

$$V_c = 36 + 324 = 360cm^3$$

But generally, volume $V = dLw = V_c$

Where d=depth, L= length, w= width

The thickness of the sample for test should be 0.32cm which will be the depth, d

$$V = 0.32Lw$$

For a square mould, $L = w = L_i$

L_i= internal length/width of the mould

$$\therefore V = 0.32L_i^{\,2} = 360cm^3$$

$$L_i^{\,2} = \frac{360}{0.32}$$

$$L_i = 33.541cm$$

Due to shrinkage, 33.7cm now becomes the internal length and width of the mould.

Taken the thickness of the mould to be 2cm, the external length and width of the mould will be;

$$L_e = L_i + 2(2)$$
$$L_e = 33.7 + 4$$
$$L_e = 37.7cm$$

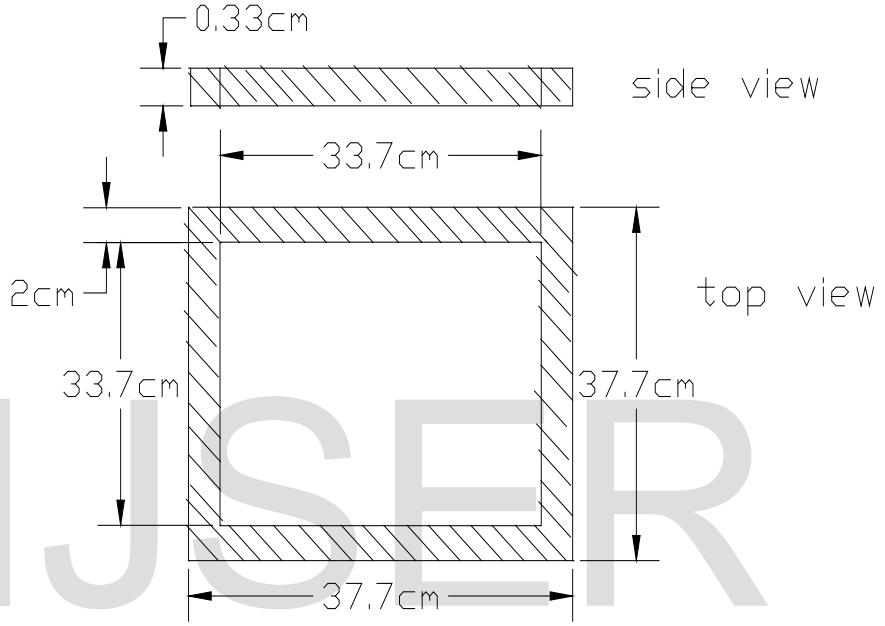

Figure 2: The mould

In this work, PWS was used to reinforce polyester resin and the effects of its different particle sizes on the mechanical properties were investigated. Most previous work done in this field focused on weight fraction in determining the filler content. The objectives of this work are to study of the mechanical properties (tensile, flexural, impact and hardness) of the periwinkle shells reinforced polyester composite (PRPC) with respect to particle sizes and volume fractions. Also to evaluate the effect of the particle sizes and volume fractions of periwinkle shells as a reinforcing agent and to identify the maximum mechanical properties of PRPC. The significance of this work is to introduce a new composite material for the material industry and also help in the waste management by recycling PWS which litters the environment. Analysis of the mechanical test result of PRPC with Minitab software 2007.

2. MATERIAL AND METHODS

2.1 Experimental Procedure

The studied composite material consists of polymer resins and filler. The raw materials used to produce the specimens are unsaturated polyester with the addition of methyl ethyl ketone

peroxide and cobalt nephthenate which served as catalyst and accelerator respectively and the grounded periwinkle shells as the filler. PWS is a waste product generated from the consumption of a small greenish-black marine snail (periwinkle), housed in a V shaped spiral shell, found in many coastal communities within Nigeria and word-wide, it is a very strong, hard and brittle material. The PWS was purchased from the local market at Port Harcourt, Nigeria. They were ground at the New market Enugu. Polyester is produced when dihydric alcohol like ethylene glycol reacts with an aromatic acid like phthalic acid to produce a polymeric ester. The typical polyester used has the physical and mechanical properties as follows; a density of $1.23gcm^{-3}$, melting point of $154^{o}c$, tensile strength of 45Mpa, Young modulus of 1.3Gpa. It was sourced commercially.

Methyl ethyl ketone peroxide (MEKP) is organic peroxide, a high explosive similar to acetone peroxide. MEKP is colorless, and in oily liquid form. MEKP is slightly less sensitive to shock and temperature, and more stable in storage. It is a substance added to a polyester resin in specific quantities to allow the polyester to cure (harden).When mixing MEKP with resin, care was taken to avoid a violent mixing action which can cause splash out of the mixing container. A measuring cup was used and not syringes as it can be shot into the container and bounce back into the eyes. It was ensured that it mixes thoroughly and methodically into the resin otherwise some portions of resin may not be catalyzed and thus not cure properly. Methyl ethyl ketone peroxide (MEKP) was sourced commercially. Cobalt II Ethyl Hexanoate (acid) was used as polyester initiator and accelerator in the production of the composite. Cobalt II Ethyl Hexanoate was sourced commercially. Paraffin wax was as a releasing agent for the mould. Paraffin wax was sourced commercially. The mould consists of four 377mm x 20mm x 4mm mild steel stick and two 377mm x 377mm x 3.2mm galvanized metal sheets. They were obtained from a metal dealer at Nsukka, Enugu State, Nigeria.

3. Volume Fraction

The volume fraction is the part or proportion of a particular element that makes up the whole volume of a composite. Calculations of volume fraction of PRPC are achieved following the derivations from the rule of mixtures based on the procedures of and implementation of Archimedes principle.

4. Determination of volume of PWS

The volumes of PWS filler are determined with the implementation of Archimedes principle [23]. Using the principle that the volume of water displaced is equivalent to the volume of submerged object [24], we can determine the volumes of the fillers with the following steps;

Step 1: The mass of a sizable quantity of ground periwinkle shells (PWS) filler lump sample is determined using digital metric system with balance (Precision: 0.0001g) and then a small container of known or previously determined density and mass, is used to contain the fillers ensuring that the small container is completely filled with PWS filler.

Step 2: A graduated glass cylinder was then filled with about 200 ml of water.

Step 3: Errors due to parallax was avoided by viewing the meniscus from a 180 degree angle, that is held up to eyes and then take the water volume measurement from the base of the curved water meniscus.

Step 4: The water volume from Step 3 was recorded and denoted as V_0

Step 5: The object (small container + fillers) was then placed into the cylinder. The water level will rise, noting that the object must be completely covered with water.

Step 6: Step 3 is repeated and recording the new water level as V_1.

Step 7: The volume V_0 (Step 4) was subtracted from V_1 (Step 6) to calculate the volume of the object, such that;

Small container + filler = $V_1 - V_0$

But the volume of water displaced, V_d ,

V_d = [volume of filler, V_f] + [volume of small container, V_{sc}]

Volume of filler, $V_f = V_d - V_{sc}$ (11)

Where $V_{sc} = \frac{M_{sc}}{\rho_{sc}}$

5. Rule of Mixture

The volume fractions were determined from the rule of mixtures which implies that for any composite, the mass of the composite equals the mass of the matrix and the mass of fillers;

$$M_c = M_f + M_m \quad (12)$$

Where volume, $V = \frac{M}{\rho}$

This implies that the volume of fillers V_f will be;

$$V_f = M_f / \rho_f \quad (13)$$

And also for volume of matrix, V_m

$$V_m = M_m / \rho_m \quad (14)$$

From the rule of mixture, the volume of composite, V_c

$$V_c = V_f + V_m \quad (15)$$

Where volume fraction for matrix, υ_m

$$\upsilon_m = \frac{V_m}{V_c} \quad (16)$$

Substituting for V_c from equation (15)

$$\upsilon_m = \frac{V_m}{V_f + V_m} \tag{17}$$

Also for volume fraction of filler, υ_f

$$\upsilon_f = V_f / V_c \tag{18}$$

Substituting for V_c from equation (15)

$$\upsilon_f = \frac{V_f}{V_f + V_m} \tag{19}$$

Using equation (19), and solving for V_m

$$V_m = \left(\frac{1 - \upsilon_f}{\upsilon_f} \right) V_f \tag{20}$$

Where equation (20) can be used to calculate the volume of polyester resin provided that the volume of fillers is determined by the Archimedes principle and the volume fraction decision is taken.

Applying the Archimedes principles and rule of mixture using equation (10), the following volume and mass shown in table 1. were gotten for the PWS filler;

Table 1: *Mass, Volume and Density of PWS sizes*

Mesh sizes (μm)	10%		20%		30%		40%		50%		*Density (g/cm^3)*
	M (g)	V (cm^3)	M (g)	V (cm^3)	M (g)	V (cm^3)	M (g)	V (cm^3)	M (g)	V (cm^3)	
400	45.5	36	91	72	136.5	108	182	144	227.5	180	*1.26*
600	45	36	90	72	135	108	180	144	225	180	*1.25*
766	44.6	36	89.2	72	133.8	108	178.4	144	223	180	*1.24*
1180	43.6	36	87.2	72	130.8	108	174.4	144	218	180	*1.21*
1760	42.2	36	84.4	72	126.6	108	168.8	144	211	180	*1.17*

By taking the mean of density in Table 1, we have the density of PWS to be approximately 1.23g/cm^3.

6. Sample Production

Sample production involves the process and procedure in the production of the PRPC. It involves the filler preparation and the composite production. The periwinkle shells were ground

in the grinding machine, then sun dried, and thereafter, classified by sieving using hand sieves and the following particle sizes were obtained: 400, 600, 766, 1180 and 1760μm. A sample of ground PWS is shown on figure 3.

Figure 3: Ground Periwinkle shells

The compression mould technique was employed in producing the composite laminates used in this work where a mild steel mold of dimension; 377×377×3.2 (in millimeter) was used for casting the composites. The mould was sun dried and then polished with a dried cloth. Then the releasing agent (parafin wax) was uniformly applied on the walls of the mould with the help of a brush. In the mixture preparation, five different particle sizes of ground periwinkle shell were used. Appropriate quantities of periwinkle shells were determined using the Archimedes's principle and added with proportionate amounts of polyester resin to give: 10%, 20%, 30%, 40% and 50% volume fractions of periwinkle shell particles. The mixture was vigorously stirred to ensure homogeneous dispersion of the periwinkle particles in the resin after the additions of methyl ethyl ketone peroxide and cobalt nephthenate which served as catalyst and accelerator respectively during curing of the polyester resin to give a solid laminate. At the time of curing, a compressive pressure of 0.05MPa was applied and the composite specimens were cured for 24 hours. Table 2 shows the volume content for each sample. Replicate samples of PWS filler reinforced polyester matrix were then subjected to tensile, flexural, impact and hardness tests. Figures 4 and 5 showed samples of the specimen ready for test and after test respectively.

Table 2: Volume percent of filler content for each particle size category of specimens

Particle sizes μm	Specimen1		Specimen2		Specimen3		Specimen4		Specimen5	
	V_p %	V_m %	V_p %	V_m %	V_p %	V_m %	V_p %	V_m %	V_p %	V_m %
400	10	90	20	80	30	70	40	60	50	50
600	10	90	20	80	30	70	40	60	50	50
760	10	90	20	80	30	70	40	60	50	50
1180	10	90	20	80	30	70	40	60	50	50
1760	10	90	20	80	30	70	40	60	50	50

Figure 4: sample for test

Figure 5: Samples after tensile test

7. Mechanical Test of the Composite

Samples of these engineering materials are subjected to a wide variety of mechanical tests to measure their strength, elastic constants, and other material properties as well as their performance under a variety of actual use conditions and environments. Each material has a property profile. The results of the material tests are used for two primary purposes: 1, engineering design (for example, failure theories based on strength, or deflections based on elastic constants and component geometry) and 2, quality control either by the materials producer to verify the process or by the end user to confirm the material specifications. The following sections contain information about mechanical tests in general as well as tension, hardness, flexural, and impact tests in particular.

Mechanical tests (as opposed to physical, electrical, or other types of tests) often involve the deformation or breakage of samples of material (called test specimens or test pieces). Note that test specimens are nothing more than specialized engineering components in which a known stress or strain state is applied and the material properties are inferred from the resulting mechanical response. More complex geometries can be used to produce conditions resembling those in actual engineering components.

When the load is removed, the specimen shortens by an amount equal to the stress divided by elastic modulus (Young's modulus). Tensile strength is calculated by dividing the load at break by the original minimum cross-sectional area [25].

8. Tensile Test

The tension test is the commonly used test for determining the tensile properties of materials using Hounsfield Tensometer (courtesy of civil engineering laboratory, UNN). Results of tension tests are tabulated in handbooks and, through the use of failure theories, these data can be used to predict failure of parts subjected to more generalized stress states. Theoretically, this is a good test because of the apparent simplicity with which it can be performed and because the uniaxial loading condition results in a uniform stress distribution across the cross section of the test specimen. Tensile strength is the maximum tensile stress a material can withstand before failure. It is a feature of the engineering stress-strain curve and cannot be found in the true strain-true stress curve. The testing machine for this test is shown in figure 2B which is a universal testing machine.

When reporting the strength of materials loaded in tension, it is customary to account for the effect of area by dividing the breaking load by the cross-sectional area:

$$\sigma = \frac{P}{A} \tag{21}$$

Where σ is the ultimate tensile stress, P is the load at fracture, and A is the cross-sectional area. (Some materials exhibit substantial reductions in cross-sectional area as they are stretched, and using the original rather than final area gives the engineering strength.) The units of stress are obviously loaded per unit area, Nm^{-2} (also called Pascals, or Pa).

Hook [26] made a number of such measurements on long wires under various loads, and observed that to a good approximation the load P and its resulting deformation δ were related linearly as long as the loads were sufficiently small. This relation, generally known as Hooke's Law, can be written algebraically as;

$$P = k\delta \tag{22}$$

Where k is the constant of proportionality called the stiffness, the units are $lbin^{-1}$ or Nm^{-1}.

A useful way to adjust the stiffness so as to be a purely materials property is to normalize the load by the cross-sectional area; i.e. to use the tensile stress rather than the load. Further, the deformation δ can be normalized by noting that an applied load stretches all parts of the wire uniformly, so that a reasonable measure of "stretching" is the deformation per unit length:

$$\varepsilon = \frac{\delta}{L} \tag{23}$$

Here L is the original length and ε is a dimensionless measure of stretching called the strain. Using these more general measures of load per unit area and displacement per unit length, Hooke's Law becomes:

$$\frac{P}{A} = E\frac{\delta}{L} \tag{24}$$

or

$$\sigma = E\varepsilon \tag{25}$$

The constant of proportionality E, called Young's modulus or the modulus of elasticity is one of the most important mechanical descriptors of a material. It has the same units as stress, Pa or psi.

The tensile tests of the composites were done using Hounsfield Tensometer model with magnification of 4:1 and 50N beam force. The cross head speed is 1 mm/min. Samples were cut from the moulded sheet into a rectangular shape with dimensions 160mm × 19mm × 3.2mm. Each specimen will be loaded to failure and the force - extension curve was plotted automatically by the equipment. The ultimate tensile strength and elastic modulus of the samples were thereafter determined from the plot.

9. Flexural Test

Also known as modulus of rupture, bend strength, or fracture strength, a mechanical parameter for brittle material, is defined as a material's ability to resist deformation under load. It is the maximum surface stress in a bent beam at the instant of failure. One might expect this to be

exactly the same as the strength measured in tension but it is larger by a factor of 1.3 because the volume subjected to this maximum stress is small, and the probability of a large flaw lying in the highly stressed region is also small. The flexural strength represents the highest stress experienced within the material at its moment of rupture. The flexural strength would be the same as the tensile strength if the material were homogeneous. Therefore it is common for flexural strengths to be higher than tensile strengths for the same material. Conversely, a homogeneous material with defects only on its surfaces (e.g. due to scratches) might have a higher tensile strength than flexural strength.

Three point bend tests were performed on the Hounsfield Tensometer to measure flexural properties. The samples were 300mm long, 19mm wide and 3.2mm thick. A three-point bend was chosen because it requires less material for each test and eliminates the need to accurately determine center point deflections with test equipment.

The flexural strength, σ_f which is the maximum stress at break, is calculated using Equation (26):

$$\sigma_f = \frac{M_b}{K} \tag{26}$$

Where σ_f the flexural strength, M_b is the maximum bending moment in the specimen, K is the cross-sectional coefficient.
Taking the moment:

$$M_b = \frac{F}{2}\frac{L}{2} = \frac{FL}{4} \tag{27}$$

Also the cross-sectional coefficient K:

$$K = \frac{bh^2}{6} \tag{28}$$

After simplifying the expression we have;

$$\sigma_f = \frac{3FL}{2bh^2} MPa \tag{29}$$

Where F is the breaking force in Newton; L is the support distance in mm; b is the width of specimen in mm; h is the thickness of specimen in mm.
Flexural stress at conventional deflection:

For the flexural strain; $\varepsilon_f = \frac{6Dd}{L^2}$ (30)

Where d is the depth of tested sample (mm) and D is the maximum deflection of the center of the sample (mm)

Flexural modulus: By calculating flexural modulus E_f the starting point is the differential equation of the neutral axis, which is in our case:

$$y'' \approx \frac{1}{R} = \frac{M}{IE_f} \tag{31}$$

Where I is the second moment, solving the equation gives Equation (3.24):

$$f = \frac{FL^3}{48IE_f} \tag{32}$$

Where f is the deflection, by regrouping this equation and substitutes this

$I = \frac{bh^3}{12}$ for the second moment ,

We now obtain Equation (33), which is the equation appearing in the standards:

$$E_f = \frac{L^3}{4bh^3}\frac{\Delta F}{\Delta f} Mpa \tag{33}$$

Where L is the support distance in mm; b is the width of specimen in mm; h is the thickness of specimen in mm; $\Delta F/\Delta f$ is the slope of the force-deflection curve. But generally this curve is not straight. We take this nonlinearity into consideration in the determination of Δf and ΔF.

10. Impact Test

This is the measure of the material toughness. Toughness is the material ability to absorb energy without rupturing. The static properties of materials and their attendant mechanical behavior are very much functions of factors such as the heat treatment the material may have received as well as design factors such as stress concentrations.

The behavior of a material is also dependent on the rate at which the load is applied. Polymeric materials and metals which show delayed yielding are most sensitive to load application rate. In design applications, impact situations are frequently encountered, such as cylinder head bolts, in which it is necessary for the part to absorb a certain amount of energy without failure. In the static test, this energy absorption ability is called "toughness" and is indicated by the modulus of rupture. A similar "toughness" measurement is required for dynamic loadings; this measurement is made with a standard ASTM impact test known as the Izod or Charpy test.

Charpy impact test specimens were used to measure the impact strength. The specimens were 63.5mm long, 7mm deep and 10mm wide. A sharp file with included angle of 45^o was drawn across the center of the saw cut at 90^o to the sample axis to obtain a consistent starter crack. The samples were fractured in a plastic impact testing machine and the impact toughness was calculated from the energy absorbed and the sample width.

11. Hardness Test (Brinell Test)

In the field of engineering, hardness is often defined as the resistance of a materials surface to abrasion, scratching and indentation (local plastic deformation). It is often measured by pressing a pointed diamond or hardened steel ball into the surface of the material. Methods to characterize hardness can be divided into three primary categories:

1) Scratch Tests

2) Rebound Tests
3) Indentation Tests

Scratch tests commonly involve comparatively scratching progressively harder materials.

Rebound tests may employ techniques to assess the resilience of material by measuring changes in potential energy.

Indentation tests actually produce a permanent impression in the surface of the material. The force and size of the impression can be related to a quantity (hardness) which can be objectively related to the resistance of the material to permanent penetration. Because the hardness is a function of the force and size of the impression, the pressure (and hence stress) used to create the impression can be related to both the yield and ultimate strengths of materials. Several different types of hardness tests have evolved over the years. These include macro hardness test such as Brinell, Vickers, and Rockwell and micro hardness tests such as Knoop and Tukon.

In this test, a large steel ball of 10 mm in diameter is used with an applied force of 500kg. The Brinell hardness number (BHN) is obtained by dividing the applied force, P, in kg, by the actual surface area of the indentation which is a segment of a sphere, such that:

$$BHN = \frac{P}{\pi Dt} = \frac{2P}{\pi D\left[D - \sqrt{\left(D^2 - d^2\right)}\right]} \quad (34)$$

Where D is the diameter of the ball in mm; t is the indentation depth from the surface in mm, and d is the diameter of the indentation at the surface in mm

12. RESULTS AND DISCUSSION

Tensile Strength: In accordance to (ASTM) D638, Hounsfield Tensometer model was used. The testing machine has a magnification of 4:1, 31.5kgf beam force, and a cross head speed of 1 mm/min. Samples were cut from the moulded sheet into a rectangular shape with dimensions 160mm × 19mm × 3.2mm. . The unit area of the sample is 60.8mm^2 which is used to calculate the tensile strength, with the initial length of 160mm^2 , the strain was also calculated and then the elastic modulus using equation (23), (25), and (27) which are presented in Table 3 – 6.

Table 3: Tensile test (particle sizes) results

(i) for 10% of PWS

Particle size (μm)	Load (N)	Extension. e (mm)	Stress σ (MPa)	Strain ε (10^{-3})	Young modulus E (GPa)
400	930	1.125	15.2961	7.0313	2.1754
600	635	1.5	10.444	9.375	1.114
766	550	1.375	9.0461	8.5938	1.0526
1180	416.6667	0.5	6.8531	3.125	2.193
1760	406.25	1.125	6.6817	7.0313	0.9503

(ii) 20% of PWS

Particle size (µm)	Load (N)	Extension. e (mm)	Stress σ (MPa)	Strain ε (10^{-3})	Young modulus E (GPa)
400	1000	1.375	16.4474	8.5938	1.9139
600	740	1.375	12.1711	8.593	1.4163
766	570	1.1	9.375	6.875	1.3637
1180	566.6667	0.875	9.375	5.4688	1.7042
1760	450	0.7083	7.4013	4.4271	1.6718

(iii) 30% of PWS

Particle size (µm)	Load (N)	Extension. e (mm)	Stress σ (MPa)	Strain ε (10^{-3})	Young modulus E (GPa)
400	1478.125	2.8906	24.3113	18.0664	1.3457
600	756.25	1.75	12.4383	10.9375	1.1989
766	655	1.4	10.7730	8.75	1.2312
1180	583.333	0.7813	9.5943	4.8825	1.965
1760	525	1.5313	8.6349	9.5706	0.9022

(iv) 40% of PWS

Particle size (µm)	Load (N)	Extension. e (mm)	Stress σ (MPa)	Strain ε (10^{-3})	Young modulus E (GPa)
400	820.8333	1.125	13.5005	7.0313	1.8518
600	500	1.2917	8.2237	8.0729	1.0187
766	475	0.75	7.8125	4.6875	1.6667
1180	408.3333	0,5833	6.716	3.6458	1.8421
1760	383.3333	1.2083	6.3048	7.5521	0.8348

(v) 50% of PWS

Particle size (µm)	Load (N)	Extension. e (mm)	Stress σ (MPa)	Strain ε (10^{-3})	Young modulus E (GPa)
400	791.6667	1.4583	13.0203	17.3177	0.7519
600	475	2.875	7.8125	9.1146	0.8571
766	433.3333	0.542	7.1272	3.3815	2.104
1180	333.333	0.5417	5.4825	3.3854	1.6194
1760	325	0.5625	5.3454	3.5156	1.5205

Table 4: Flexural test (particle sizes) results

(i) 10% of PWS

Particle sizes(μm)	Load (N)	Deflection d (mm)	Flexural Strain ε_f (10^{-3})	Flexural Strength σ_t (MPa)	Flexural Modulus E_f (GPa)
400	13.65	4.6875	1	31.5712	31.5712
600	9.45	4.65	0.992	21.857	22.0333
766	8.1375	3.7083	0.7911	18.8213	23.7913
1180	9.45	6.7912	1.4489	21.857	15.0852
1760	8.505	4.05	0.864	19.6713	22.7677

(ii) 20% of PWS

Particle sizes(μm)	Load (N)	Deflection d (mm)	Flexural Strain ε_f (10^{-3})	Flexural Strength σ_t (MPa)	Flexural Modulus E_f (GPa)
400	15.3	5.0271	1.0725	35.3875	32.9954
600	11.8125	3.875	0.8267	27.3213	33.0486
766	8.6625	4.5625	0.9733	20.0356	20.5852
1180	11.97	4.65	0.992	27.6855	27.9088
1760	9	7.7143	1.6457	20.8162	12.6488

(iii) 30% of PWS

Particle sizes(μm)	Load (N)	Deflection d (mm)	Flexural Strain ε_f (10^{-3})	Flexural Strength σ_t (MPa)	Flexural Modulus E_f (GPa)
400	20.475	4.75	1.0133	47.3569	46.7333
600	13.86	2.85	0.608	32.0569	52.7252
766	13.125	5.9375	1.2667	30.357	23.9654
1180	12.075	2.625	0.56	27.9284	49.8721
1760	9.975	3.2708	0.6978	23.0713	33.0629

(iv) 40% of PWS

Particle sizes(μm)	Load (N)	Deflection d (mm)	Flexural Strain ε_f (10^{-3})	Flexural Strength σ_t (MPa)	Flexural Modulus E_f (GPa)
400	8.6625	2.0938	0.4467	24.0427	33.4298
600	8.6625	3.8125	0.8133	20.0356	24.6349
766	7.56	2.625	0.56	17.4856	31.2243
1180	7.0875	5.2083	1.1111	16.3928	14.7536
1760	5.67	4.1	0.8747	13.1142	14.992

(v) 50% of PWS

Particle sizes(μm)	Load (N)	Deflection d (mm)	Flexural Strain ε_f	Flexural Strength σ_t	Flexural Modulus E_f

			(10^{-3})	(MPa)	(GPa)
400	12.6	4.875	1.04	20.0356	28.02180858
600	5.25	5.625	1.2	12.1428	10.119
766	6.3	4.5	0.96	15.3	15.17847965
1180	6.3	3	0.64	14.5713	22.7677
1760	5.5125	2.2188	0.4733	12.7499	26.9385

Table 5: Hardness test results (Brinell hardness number BHN)

For 1760µm size

SN	% Filler content	d_m(mm)	d (d_m/4)(mm)	$e=\sqrt{(D^2-d^2)}$	$c=\pi D(D-e)$	$BHN=\frac{2p}{c}$
1	10	8	2	0	12.5664	33
2	20	10	2.5	1.5	3.1416	52
3	30	7	1.75	0.9682	8.0546	65
4	40	6.5	1.625	1.1659	5.2407	80
5	50	10	2.5	1.5	3.1416	134

For 1180µm size

SN	Filler conteny%	d_m(mm)	d_r(d_m/4)(mm)	$e=\sqrt{(D^2-d^2)}$	$c=\pi D(D-e)$	$BHN=\frac{2p}{c}$
1	10	8	2	0	12.5664	33
2	20	7.5	1.875	0.696	8.1935	51
3	30	6.5	1.625	1.1659	5.2407	80
4	40	6	1.5	1.3229	4.2545	99
5	50	13	3.25	2.5617	3.5295	119

For 766µm size

SN	Filler conteny%	d_m(mm)	d_r(d_m/4)(mm)	$e=\sqrt{(D^2-d^2)}$	$c=\pi D(D-e)$	$BHN=\frac{2p}{c}$
1	10	7	1.75	0.9682	6.4827	65
2	20	7	1.75	0.9682	6.4827	65
3	30	6.5	1.625	1.1659	5.2407	80
4	40	6	1.5	1.3229	4.2545	99
5	50	6	1.5	1.3229	4.2545	99

For 600µm size

SN	Filler conteny%	d_m(mm)	d_r(d_m/4)(mm)	$e=\sqrt{(D^2-d^2)}$	$c=\pi D(D-e)$	$BHN=\frac{2p}{c}$
1	10	8	2	0	12.5664	33
2	20	7	1.75	0.9682	6.4827	65
3	30	9	2.25	1.0308	6.0898	69
4	40	6.5	1.625	1.1659	5.2407	80
5	50	4.5	1.125	1.6536	2.1765	193

For 400µm size

SN	Filler conteny%	d_m(mm)	$d_r(d_m/4)$(mm)	$e=\sqrt{(D^2-d^2)}$	$c=\pi D(D-e)$	$BHN=\frac{2p}{c}$
1	10	8	2	0	12.5664	33
2	20	7	1.75	0.9682	6.4827	65
3	30	6.5	1.625	1.1659	5.2407	80
4	40	9.5	2.375	1.2809	4.5184	93
5	50	4	1	1.7321	1.6836	249

Table 6; Summary Results for Hardness Test

Filler content	400µm	600µm	766µm	1180µm	1760vm
10%	33	33	65	33	33
20%	65	65	65	51	52
30%	80	69	80	80	65
40%	93	80	99	99	80
50%	249	193	99	119	134

Table 7: Impact test results

Filler content	400**µm**	600**µm**	766**µm**	1180**µm**	1760**µm**
10%	6.3	6.7	7.1	7.9	9.0
20%	8.5	9.1	9.8	11.2	13.2
30%	9.5	10.2	10.9	12.3	14.3
40%	16.5	17.4	18.3	20.1	22.7
50%	17.0	17.9	18.8	20.6	23.2

Note that all dimensions are in Jm^{-2}

13. Tensile Strength on particle sizes

The response of tensile strength against the particle sizes for 10%, 20%, 30%, 40% and 50% content as shown in figure 6.

For 10% PWS filler content, it was observed that 400µm particle size has tensile strength of 15. 3MPa, it decreases to 10.5MPa at 600µm particle size. At 766µm particle size the tensile strength reads 9.1MPa while at 1180µm particle size the strength reads 6.8MPa. The last largest particle size which is 1760µm reads 6.7MPa. it can be observed that the maximum tensile strength of 15.3MPa was gotten at 400µm particle size and the minimum of 6.7MPa at 1760µm particle size. The slope of 10% filler content shows that increase in particle size decreases the tensile strength of the composite material.

For 20% PWS filler content, it was observed that 400µm particle size has tensile strength of 16.5MPa, it decreases to 12.2MPa at 600µm particle size. At 766µm particle size the tensile strength reads 9.4MPa while at 1180µm particle size the strength reads 9.3MPa. The last largest

particle size which is 1760µm reads 7.4MPa. It can be observed that the maximum tensile strength of 16.5MPa was gotten at 400µm particle size and the minimum of 7.4MPa at 1760µm particle size. The slope of 20% filler content shows that increase in particle size decreases the tensile strength of the composite material.

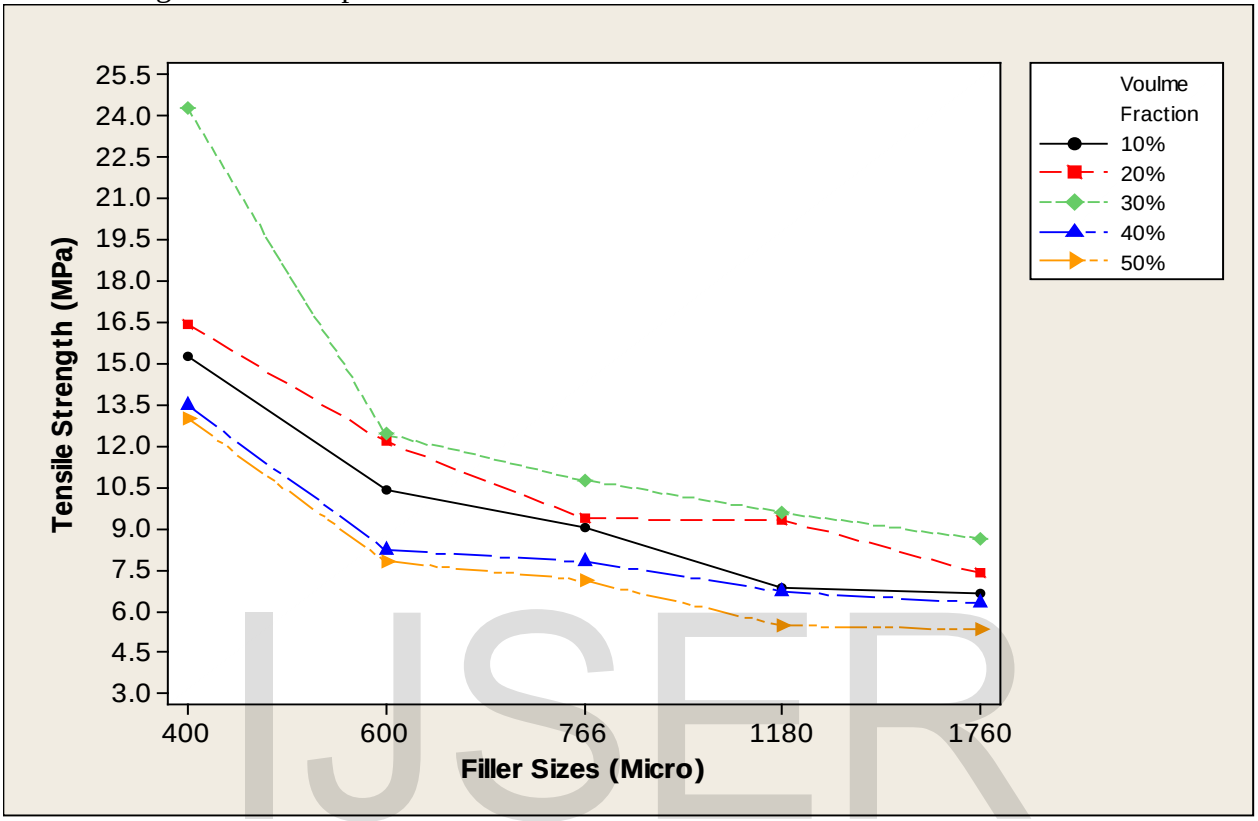

Figure 6: Effect of particle size on tensile strength for 10% - 50% content

For 30% PWS filler content, it was observed that 400µm particle size has tensile strength of 24. 3MPa, it decreases to 12.4MPa at 600µm particle size. At 766µm particle size the tensile strength reads 10.8MPa while at 1180µm particle size the strength reads 9.6MPa. The last largest particle size which is 1760µm reads 8.6MPa. It can be observed that the maximum tensile strength of 24.3MPa was gotten at 400µm particle size and the minimum of 8.6MPa at 1760µm particle size. The slope of 30% filler content shows that increase in particle size decreases the tensile strength of the composite material.

For 40% PWS filler content, it was observed that the smallest particle size of 400µm has tensile strength of 13.5MPa. It decreases to 8.2MPa at 600µm particle size. At 766µm particle size the tensile strength reads 7.8MPa while at 1180µm particle size the strength reads 6.7MPa. The last largest particle size which is 1760µm reads 6.3MPa. It can be observed that the maximum tensile strength of 13.5MPa was gotten at 400µm particle size and the minimum of 6.3MPa at 1760µm particle size. The slope of 40% filler content shows that increase in particle size decreases the tensile strength of the composite material.

For 50% PWS filler content, it was observed that the smallest particle size of 400µm has tensile strength of 13MPa. It decreases to 7.8MPa at 600µm particle size. At 766µm particle size the tensile strength reads 7.1MPa while at 1180µm particle size the strength reads 5.5MPa. The last largest particle size which is 1760µm reads 5.3MPa. It can be observed that the maximum tensile

strength of 13MPa was gotten at 400μm particle size and the minimum of 5.3MPa at 1760μm particle size. The slope of 50% filler content shows that increase in particle size decreases the tensile strength of the composite material.
Generally, all the slopes show that increase in particle sizes decreases the tensile strength of the composite materials. It is observed that particle size of 400μm of all the filler content gave the highest strength. This is in agreement with the finding of Njoku et al (2011) on the work; effects of variation of particle size and weight fraction on the tensile strength and modulus of reinforced polyester composite. The optimum tensile strength was observed to be 24.3MPa on 30% slope.

For 766μm PWS particle size, it was observed that the lowest filler content of 10% has tensile strength of 9MPa. It increases to 9.3MPa at 20% filler content. At 30% filler content, the tensile strength reads 10.8MPa while at 40% filler content the strength reads 7.8MPa. The last highest filler content 50% reads 7.1MPa. It can be observed that the maximum tensile strength of the slope 10.8MPa was gotten at 30% filler content and the minimum of 7.1MPa at 50% filler content. The slope of 1760μm particle size PRPC shows that the tensile strength increases from 10% to 30% filler content, then decreases from 30% to 50%.
For 600μm PWS particle size, it was observed that the lowest filler content of 10% has tensile strength of 10.4MPa. It increases to 12.2MPa at 20% filler content. At 30% filler content, the tensile strength reads 12.4MPa while at 40% filler content the strength reads 8.2MPa. The last highest filler content 50% reads 7.8MPa. It can be observed that the maximum tensile strength of the slope 12.4MPa was gotten at 30% filler content and the minimum of 7.8MPa at 50% filler content. The slope of 1760μm particle size PRPC shows that the tensile strength increases from 10% to 30% filler content, then decreases from 30% to 50%.

For 400μm PWS particle size, it was observed that the lowest filler content of 10% has tensile strength of 15.3MPa. It increases to 16.4MPa at 20% filler content. At 30% filler content, the tensile strength reads 24.3MPa while at 40% filler content the strength reads 13.5MPa. The last highest filler content 50% reads 13MPa. It can be observed that the maximum tensile strength of the slope 24.3MPa was gotten at 30% filler content and the minimum of 13MPa at 50% filler content. The slope of 1760μm particle size PRPC shows that the tensile strength increases from 10% to 30% filler content, then decreases from 30% to 50% filler content.

All the slopes show that there is increase in tensile strength as filler content increases from 10% to 30%, but decreases from 30% to 50%. It is observed that filler content of 30% of all the particle sizes gave an improved strength. This is in agreement with the finding of Ofem et al (2011); Effect of filler content on the mechanical properties of periwinkle shell reinforced cashew nut shell liquid (CNSL) resin composites. The optimum tensile strength was observed to be 24.3MPa on 30% slope.

14. Flexural Strength

Three point bend tests will be performed in accordance with ASTM D790M test method 1(procedure A) to measure flexural properties. The samples were 300mm long, 19mm wide and 3.2mm thick.
The flexural strength, strain and modulus of the samples which were determined using equations (31), (32) and (33) respectively as shown in Table 6 – 9.

Flexural Strength on particle sizes: The response of the flexural strength against the particle sizes at 10%, 20%, 30%, 40% and 50% content as shown in figure 7;

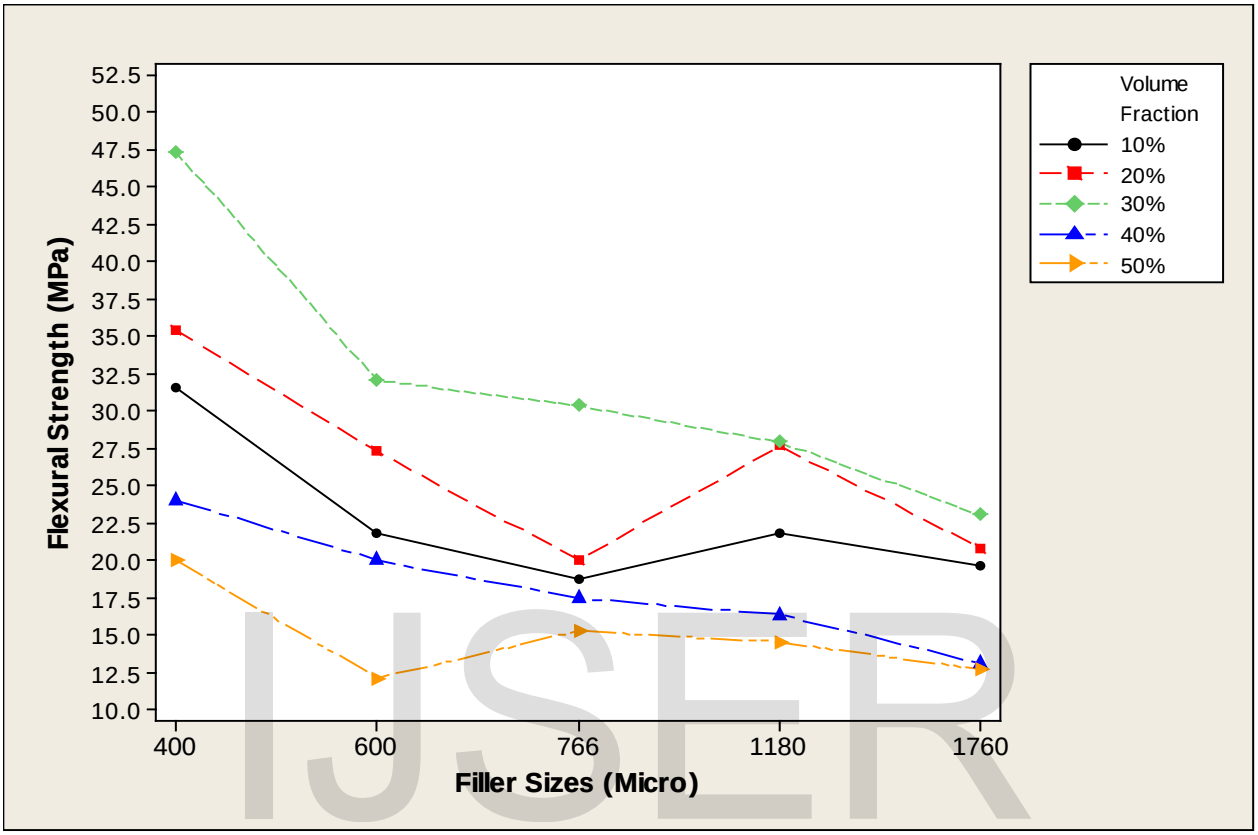

Figure 7: Effect of particle size on flexural strength for 10% - 50% content.

Figure 7shows the plot of flexural strength against particle sizes with the slopes of 10%, 20%, 30%, 40% and 50% content.

For 10% PWS filler content, it was observed that the smallest particle size of 400µm has flexural strength of 31.6MPa. It decreases to 21.9MPa at 600µm particle size. At 766µm particle size the flexural strength reads 18.8MPa while at 1180µm particle size the strength reads 21.9MPa. The last largest particle size which is 1760µm reads 19.7MPa. It can be observed that the maximum flexural strength of 31.6MPa was gotten at 400µm particle size and the minimum of 19.7MPa at 1760µm particle size. The slope of 10% filler content shows that increase in particle size decreases the flexural strength of the composite material.
For 20% PWS filler content, it was observed that the smallest particle size of 400µm has flexural strength of 35.4MPa. It decreases to 27.3MPa at 600µm particle size. At 766µm particle size the flexural strength reads 20MPa while at 1180µm particle size the strength reads 27.7MPa. The last largest particle size which is 1760µm reads 20.8MPa. It can be observed that the maximum flexural strength of 35.4MPa was gotten at 400µm particle size and the minimum of 20.8MPa at 1760µm particle size. The slope of 20% filler content shows that increase in particle size decreases the flexural strength of the composite material.

For 30% PWS filler content, it was observed that the smallest particle size of 400µm has flexural strength of 47.4MPa. It decreases to 32.1MPa at 600µm particle size. At 766µm particle size the flexural strength reads 30.4MPa while at 1180µm particle size the strength reads 27.9MPa. The last largest particle size which is 1760µm reads 23.1MPa. It can be observed that the maximum flexural strength of 47.4MPa was gotten at 400µm particle size and the minimum of 23.1MPa at 1760µm particle size. The slope of 30% filler content shows that increase in particle size decreases the flexural strength of the composite material.
For 40% PWS filler content, it was observed that the smallest particle size of 400µm has flexural strength of 24MPa. It decreases to 20MPa at 600µm particle size. At 766µm particle size the flexural strength reads 17.5MPa while at 1180µm particle size the strength reads 16.4MPa. The last largest particle size which is 1760µm reads 13.1MPa. It can be observed that the maximum flexural strength of 24MPa was gotten at 400µm particle size and the minimum of 13.1MPa at 1760µm particle size. The slope of 10% filler content shows that increase in particle size decreases the flexural strength of the composite material.
For 50% PWS filler content, it was observed that the smallest particle size of 400µm has flexural strength of 20MPa. It decreases to 12.1MPa at 600µm particle size. At 766µm particle size the flexural strength reads 15.3MPa while at 1180µm particle size the strength reads 14.6MPa. The last largest particle size which is 1760µm reads 12.7MPa. It can be observed that the maximum flexural strength of 20MPa was gotten at 400µm particle size and the minimum of 12.7MPa at 1760µm particle size. The slope of 50% filler content shows that increase in particle size decreases the flexural strength of the composite material.

All the slopes show that increase in particle sizes decreases the flexural strength of the composite materials. It is observed that particle size of 400µm of all the filler content gave the highest strength. The optimum flexural strength was observed to be 24.3MPa on 30% slope.

15. Hardness Strength (Brinell Test)
The samples were indented with a universal testing machine where a large steel ball of 10 mm in diameter is used with an applied force of 500 kg according to ASTM D785and the Brinell hardness number (BHN) was calculated by substituting for the diameter of the indention made on the material in equation (34).

Hardness strength (BHN) on particle sizes: The response of the hardness strength (BHN) against the particle sizes at 10%, 20%, 30%, 40% and 50% content as shown in Figure 8.

For 10% PWS filler content, it was observed that 400µm particle size has a BHN of 33; 600µm particle size also has BHN of 33. At 766µm particle size the BHN reads 65 while at 1180µm particle size the BHN reads 33. The last largest particle size which is 1760µm reads 22. It can be observed that the maximum hardness number of 65 was obtained at 400µm particle size and the minimum of 22 at 1760µm particle size. The slope of 10% filler content shows that apart from 766µm and 1760µm all other ones have the same BHN.
For 20% PWS filler content, it was observed that 400µm particle size has a BHN of 65, 600µm particle size and 766µm particle size also has BHN of 65, while at 1180µm particle size the BHN reads 51. The last largest particle size which is 1760µm reads 52. It can be observed that the maximum hardness number of 65 was gotten at 400µm, 600µm and 766µm particle sizes and the

minimum of 51 at 1180µm particle size. The slope of 10% filler content shows that apart from 1180µm and 1760µm particle sizes, all other ones have the same BHN.

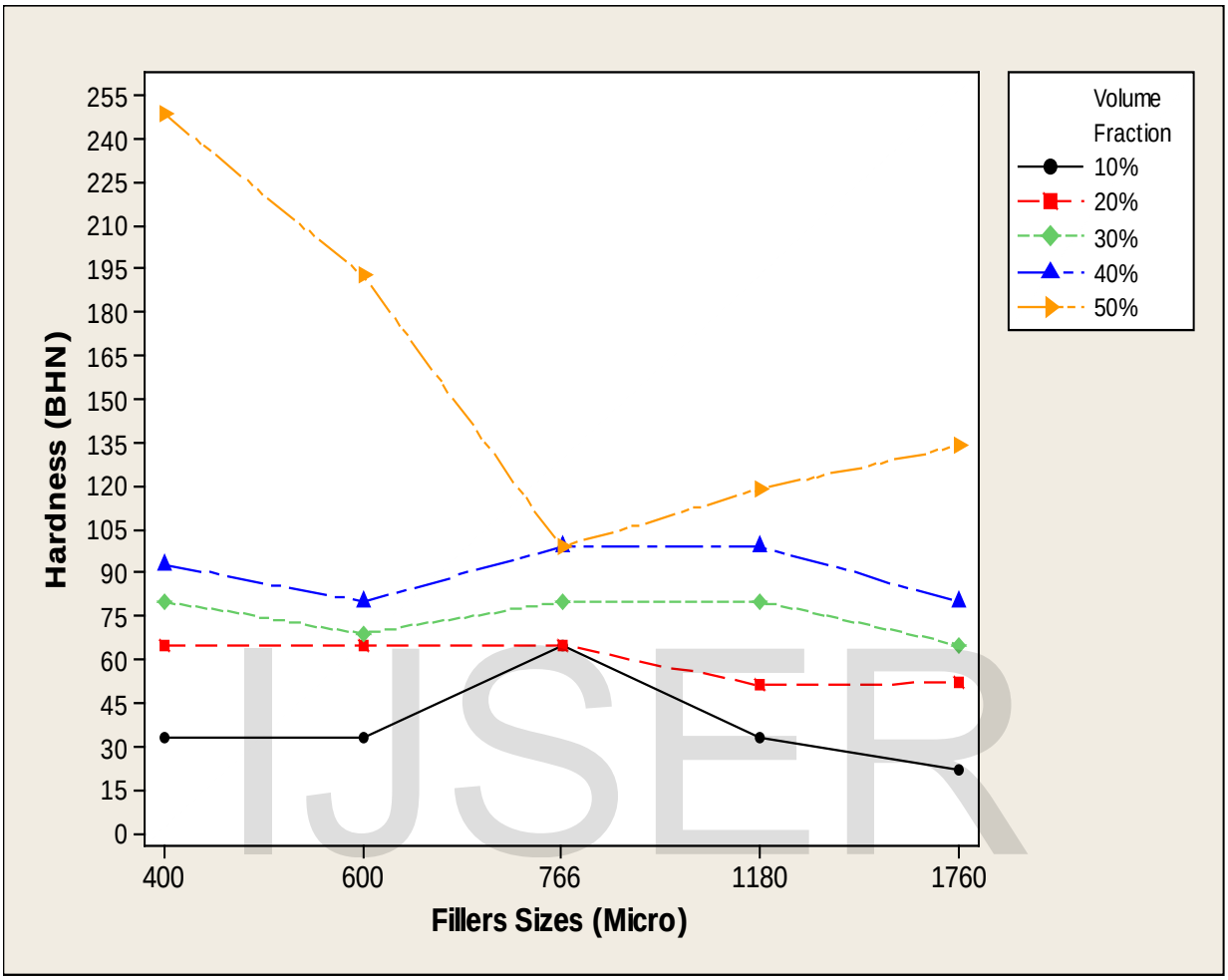

Figure 8: Effect of particle size on BHN for 10% - 50% content

For 30% PWS filler content, it was observed that 400µm particle size has a BHN of 80, 600µm particle size has BHN of 69 and 766µm particle size has BHN of 80, while at 1180µm particle size the BHN reads 80. The last largest particle size which is 1760µm reads 65. It can be observed that the maximum hardness number of 80 was gotten at 400µm, 766µm and 1180µm particle sizes and the minimum of 51 at 1760µm particle size. The slope of 10% filler content shows that apart from 600µm and 1760µm particle sizes, all other ones have the same BHN.

For 40% PWS filler content, it was observed that 400µm particle size has a BHN of 93, 600µm particle size has BHN of 80, while 766µm particle size also has BHN of 99. At 1180µm particle size, the BHN reads of 99. The last largest particle size which is 1760µm reads 80. It can be observed that the maximum hardness number of 99 was gotten at 766µm and 1180µm particle sizes and the minimum of 80 at 600µm particle size. The slope of 10% filler content shows that 1180µm and 766µm have the same BHN. Also 600µm and 1760µm has the same BHN.

For 50% PWS filler content, it was observed that 400µm particle size has a BHN of 249, 600µm particle size has 193BHN, 766µm particle size has BHN of 99, while at 1180µm particle size the BHN reads 119. The last largest particle size which is 1760µm reads 134BHN. It can be

observed that the maximum hardness number of 249 was gotten at 400µm particle size and the minimum of 99BHN at 766µm particle size. The slope of 50% filler content shows that apart from 400µm to 766µn then rises.

All the slopes except the 50% content slopes shows that increase in particle sizes decreases the hardness strength of the composite materials but rises only at 766µm particle size. The 50% content slope decreases but then rises at 1180µm and 1760µm particle size. The optimum hardness number was observed to be 249BHN on 50% slope at 400µm particle size.

16. Impact Strength

Charpy impact test specimens were prepared in accordance with ASTM D256M to measure the impact strength. The specimens were 63.5mm long, 7mm deep and 10mm wide. The impact toughness was calculated from the energy absorbed and the sample width. The impact toughness of the samples are shown in Table 5

Impact strength on particle sizes: The response of impact strength against particle sizes at 10%, 20%, 30%, 40% and 50% content as shown in Figure 9;

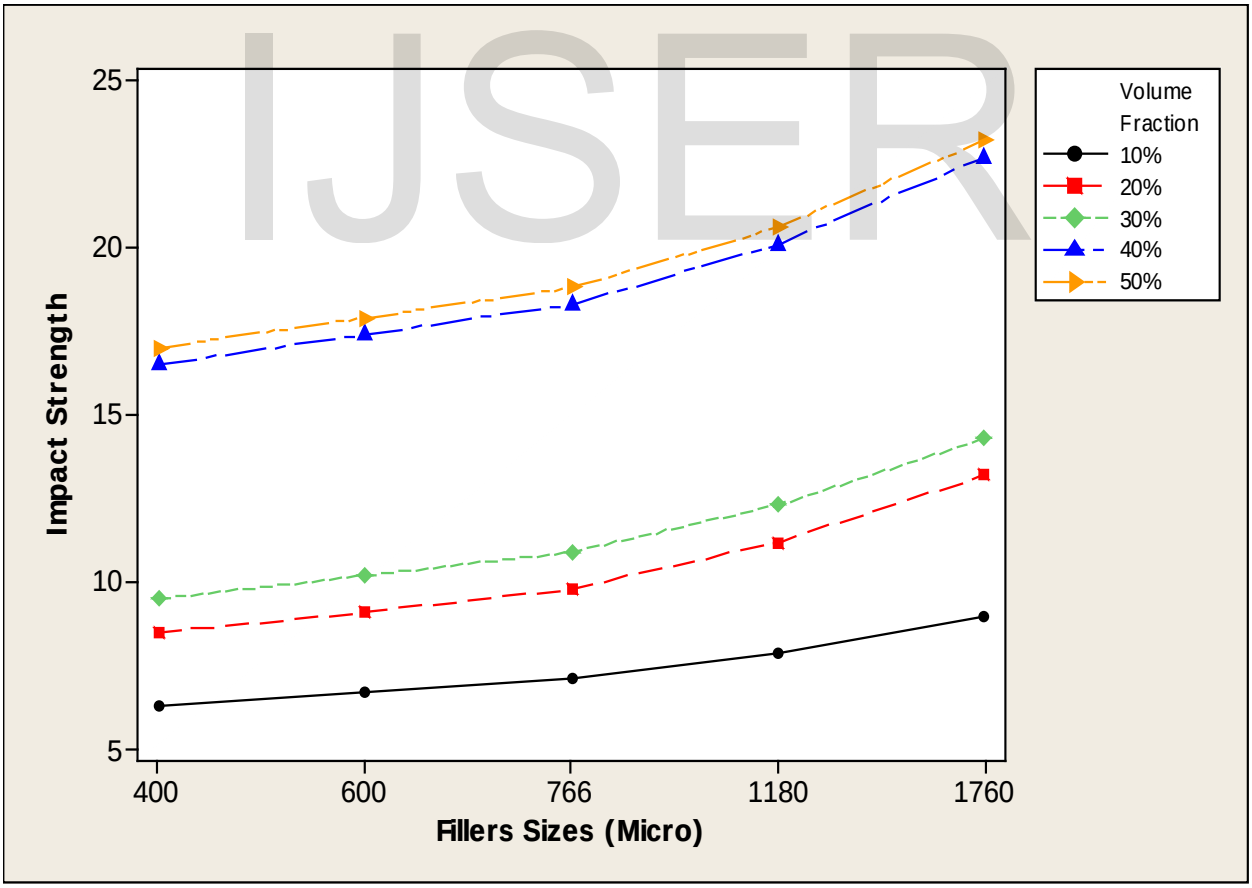

Figure 9: Effects of particle sizes on impact strength 10% -50% content

In Figure 9, effects of filler content on the impact strength of PRPC, shows that the 400µm particle size slope started at 10% content with 6.3Jm^{-2} and ends at 50% content with 17Jm^{-2}. The 600µm particle size slope started at 10% content with 6.7Jm^{-2} and ends at 50% content with 17.9Jm^{-2}. The 766µm particle size slope started at 10% content with 7.1Jm^{-2} and ends at 50% content with 18.8Jm^{-2}. The 1180µm particle size slope started at 10% content with 7.9Jm^{-2} and ends at 50% content with 20.6Jm^{-2}. The 1760µm particle size curve started at 10% content with 9Jm^{-2} and ends at 50% content with 23.2Jm^{-2}.

17. Polynomial Regression Analysis for Tensile Strength

(i) Tensile Strength versus Particle sizes (Micro)

The regression equation is;

Tensile Strength (σ) = 24.49 - 0.02704 (d) + 0.000010 $(d)^2$

S = 2.71402 R-Sq = 62.0% R-Sq(adj) = 58.5%

Analysis of Variance

Source	DF	SS	MS	F	P
Regression	2	264.158	132.079	17.93	0.000
Error	22	162.049	7.366		
Total	24	426.208			

Sequential Analysis of Variance

Source	DF	SS	F	P
Linear	1	182.586	17.24	0.000
Quadratic	1	81.572	11.07	0.003

From the regression equation above it is revealed that a unit increase in particle sizes (d) will reduce hardness by 0.02704 percent while a squared unit increase will increase it by a negligible size of 0.000010 percent. The regression furthers revealed a p-value of 0.000, which is less than the α-value of 0.05 level of significance. This indicates that the relationship between tensile strength and particle sizes is significant. This is further supported by a low standard error of 2.71402, which confirms that the sample mean is an accurate reflection of the actual data used for the study. With an F-statistic of 17.93 and a co-efficient of determination R^2(R-sq)of 62.0% it

is showed that particle sizes can account for 62.0% of the total variations in tensile strength while the remaining 38.0% is accounted for by other variables other than tensile strength.

18. Polynomial Regression Analysis for Flexural Strength

(i) Flexural Strength versus Particle sizes (Micro)

The regression equation is

Flexural Strength (σ_f) = 39.39 - 0.02960 (d) + 0.000010 $(d)^2$

S = 7.40106 R-Sq = 65.4% R-Sq(adj) = 58.6%

Analysis of Variance

Source	DF	SS	MS	F	P
Regression	2	409.82	204.908	13.74	0.040
Error	22	1205.07	54.776		
Total	24	1614.88			

Sequential Analysis of Variance

Source	DF	SS	F	P
Linear	1	322.691	15.74	0.025
Quadratic	1	87.124	11.59	0.031

The regression equation above revealed that a unit increase in particle size (d) will reduce flexural strength by 0.02960 percent while a squared unit increase will it by negligible value of 0.000010 percent. The regression further revealed a p-value of 0.040, which is less than the α-value of 0.05 level of significance. This indicates that the relationship between flexural strength and particle sizes is significant. However, the low standard error of 7.40106 and an f-statistic of 13.74 showed that the sample mean is an accurate reflection of the actual data. The co-efficient of determination R^2(R-sq) revealed by the regression is 65.4 percent, which also indicates that particle sizes could explain about 64.7 percent of the total variation in flexural strength.

19. Polynomial Regression Analysis for Hardness Strength

(i) Hardness (BHN) versus Particle sizes (Micro)

The regression equation is

Hardness (BHN) = 127.4 - 0.0757(d) + 0.000025 $(d)^2$

S = 20.6077 R-Sq = 65.2% R-Sq(adj) = 61.1%

Analysis of Variance

Source	DF	SS	MS	F	P
Regression	2	3111.5	1555.75	10.07	0.032
Error	22	56345.1	2561.14		
Total	24	59456.6			

Sequential Analysis of Variance

Source	DF	SS	F	P
Linear	1	2582.31	10.07	0.032
Quadratic	1	529.19	6.21	0.054

The regression equation above revealed that a unit increase in particle sizes (d) will reduce hardness by 0.0757 percent while a squared unit increase will increase it by a negligible size of 0.000025 percent. The regression furthers revealed a p-value of 0.032, which is less than the α-value of 0.05 level of significance. This indicates that the relationship between hardness and particle sizes is significant. This is further supported by a high standard error of 20.6077, which confirms that the sample mean is not an accurate reflection of the actual data used for the study. With an F-statistic of 10.07 and a co-efficient of determination R^2(R-sq)of 65.2% it is showed that particle sizes can account for only about 65.2% of the variations in hardness while the remaining 34.8 is accounted for by other variables other than hardness.

20. Polynomial Regression Analysis for Impact Strength

(i) Impact Strength versus Particle sizes (Micro)

The regression equation is

Impact Strength (Jm^{-2}) = - 2.471 + 0.02607 (d) - 0.000008 $(d)^2$

S = 2.19118 R-Sq = 84.2% R-Sq(adj) = 82.8%

Analysis of Variance

Source	DF	SS	MS	F	P
Regression	2	563.792	281.896	58.71	0.000
Error	22	105.628	4.801		
Total	24	669.420			

Sequential Analysis of Variance

Source	DF	SS	F	P
Linear	1	514.434	76.34	0.000
Quadratic	1	49.357	10.28	0.004

The regression equation on the relationship between impact and particle sizes above revealed a negative relationship (depicts by the negative constant of -2.471). From the regression equation, it is shown that a unit increase in particle sizes will increase Impact strength by 0.2607 (depicts by +0.2607) in the equation, while a squared unit increase in particle sizes will further reduce a negligible figure of 0.000008 (-0.000008)percent. The regression further revealed a p-value of 0.000, which is less than the α-value of 0.05 level of significance. This indicates that the relationship between impact strength and particle sizes is very significant. Similarly, the low standard error of 2.19118 and an f-statistic of 58.71 showed that the sample mean is a more accurate reflection of the actual data. The co-efficient of determination R^2(R-sq)of 84.2%, revealed that particle sizes can explain approximately, about 84 percent of the total variation in impact strength.

21. Conclusion

The effect of particle sizes on the mechanical properties of PRPC was studied and the following deductions were made using particles as fillers, which is ground periwinkle shells with sizes 1760, 1180, 766, 600, 400μm particle sizes, subjected to control factors at 50%, 40%, 30%, 20% and 10% filler content.

- Decrease in particle sizes increases the tensile strength and flexural strength, but causes a scattered diagram in hardness strength. In impact test, the strength increases with increase in particle size. For the filler content, the tensile and flexural strength rises highest at 30% content where it then decreases sharply, but in hardness and impact test, increase in filler content increases the BHN and impact strength.
- The maximum tensile strength was gotten from composite made up of 24.3MPa at 400μm particle size with 30% filler content and the minimum of 5.3MPa was obtained from 1760μm particle size at 50% filler content;
- The maximum flexural strength of 47.4MPa was obtained from the composite of 400μm particle size at 30% filler content, and the minimum of 12.7MPa was obtained from

1760µm particle size at 50% filler content, 600µm particle size at 10% filler content, 766µm particle size at 30% and 50% filler content.

- The maximum hardness number (BHN) of 249BHN was obtained from the composite of 400µm particle size at 50% filler content, the minimum of 33BHN were obtained from 400µm particle size at 10% filler content, 600µm particle size at 10% filler content, 1180µm particle size at 10% filler content and 1760µm particle size at 10% filler content.
- The maximum impact strength of 23.2Jm^{-2} was obtained from the composite made up of 1760µm particle size at 50% filler content, the minimum of 6.3Jm^{-2} were obtained from 400µm particle size at 10% filler content.

The PRPC can be applied in the design and production of automobile parts, ceiling boards, floor tiles, and furniture

REFERENCES

1. Satyanarayana, K. G., Ramos, L. P. and Wypych, F. (2005) Development of new materials based on agro and industrial wastes towards ecofriendly society. 583-624.

2. Raju, G. U., Kumarappa, S. and Gaitonde, V. N. (2012) Mechanical and physical characterization of agricultural waste reinforced polymer composites. Journal for Material Environment and Science 3 (5) 907-916

3. Imoisili, P. E., Ukoba, K.O, Ibegbulam, C. M., Adgidzi, D. and Olusunle, S.O. (2012) Effect of Filler Volume Fraction on the Tensile Properties of Cocoa-Pod Epoxy Resin Composite. International Journal of Science and Technology 2(7).

4. Wretfors, C. and Svennerstedt, B. (2006) Biofibre Technology used in military applications An overview. Journal for Biofibre Technology Rapport 142, 1 - 40

5. Ghosh, T. N., Chakrabarti T., and Tripathi, G. (2000) Biotechnology in energy management. New Delhi: APH Publishing Corporation.

6. Mohanty, A. K., Misra, M. and Hinrichsen, G. (2000) Biofibers, Biodegradable Polymers and Biocomposites: An Overview. Macromolecular Materials and Engineering 276/277, 1-24.

7. Jiken, L., Malhmmar, G. and Selden, R. (1991) The effect of mineral fillers on impact and tensile properties of polypropylene. Polymer Testing 10, 329-344.

8. Ishak, M. R., Leman, Z., S. M. Sapuan, S. M., Edeero-zey, A. M. M. and Othman, I. S. (2010) Mechanical Properties of Kenaf bast and Core Fibre Reinforced Unsaturated Polyester Composites. IOP Conference Series: Materials Science and Engineering 11(1), 1-6.

9. Kandachar, P. and Brouwer, R. (2002) Applications of Bio-composites in Industrial Production. Materials Resources Society Symposium Proceedings 702, 101 - 112.

10. Zaini, R. E., Rowell, S. M. and Sanadi, A. R. (1995) Recent developments in annual growth lignocellulosic as reinforcing fillers in thermoplastics. Proceeding of 2nd Biomass Conference of the Americas: Energy, Environment, Agriculture and Industry 1171-1180.

11. Ofem, M. I., Umar, M., and Ovat, F. A. (2012) Mechanical Properties of Rice Husk Filled Cashew Nut Shell Liquid Resin Composites. Journal of Materials Science Research 1(4), 89.

12. Egwaikhide, P.A., Akporhonor, E.E. and Okiemen, F.E. (2007) An Investigation on the Potential of Palm Karnel Husk as Fillers in Rubber Reinforcement. Middle-East Journal of Scientific Research 2 (1), 28-32,

13. Olutoge, F. A., Okeyinka, O. M., and Olaniyan, O. S., (2012) Assessment of the suitability of periwinkle shell ash (psa) as partial replacement for ordinary Portland cement (opc) in concrete. IJRRAS 10(3) www.arpapress.com/Volumes/Vol10Issue3/IJRRAS_10_3_08.pdf

14. Mmom, P. C. and, Arokoya, S. B. (2010) Mangrove Forest Depletion, Biodiversity Loss and Traditional Resources Management Practices in the Niger Delta, Nigeria. Research Journal of Applied Sciences, Engineering and Technology, 2 (1), 28-34.

15. Powell, C. B., Hart, A. I. and Deekae, S. (1985) Market Survey of the PeriwinkleTympanotonus fascatus in Rivers State: Sizes, Prices, Trade Routes and Exploitation levels. Proceedings of the 4th Annual Conference of the Fisheries Society of Nigeria (FISON), Fisheries Society of Nigeria, Port Harcourt, Nigeria, 55-61.

16. Jamabo, N. and Chinda, A. (2010) Aspects of the Ecology of Tympanotonous fuscatus var fuscatus (Linnaeus,1758) in the Mangrove Swamps of the Upper Bonny River, Niger Delta, Nigeria. Current Research Journal of Biological Sciences, 2(1), 42-47.

17. Aku, S. Y., Yawas, D.S., Madakson, P.B., and Amaren, S.G. (2012) Characterization of Periwinkle Shell as Asbestos-Free Brake Pad Materials. *The Pacific Journal of Science and Technology* 13(2), 57-63.

18. Painter, T.J. and Hemmer, P.C. (1979) The distribution of calcium carbonate layers in periwinkle and snail shells: new evidence from gastropod molhusks. Calcium carbonate Research, 69, 217 - 226.

19. Davallo, M., Pasdar, H., and Mohseni, M., (2010) "Mechanical Properties of Unsaturated Polyester Resin" International Journal of ChemTech Research 2 (4), 2113-2117.

20. Fu, S. Y., Feng, X. Q., Lauke, B., and Mai, Y. W. (2008) Effects of particle size, particle/matrix interface adhesion and particle loading on mechanical properties of particulate - polymer composite. Composites part B: Engineering 39, 933 - 961.

21. Nwanonenyi, S. C, Obidiegwu, M.U., and Onuegbu, G. C. (2013) Effects of Particle Sizes, Filler Contents and Compatibilization On The Properties Of Linear Low Density Polyethylene Filled Periwinkle Shell Powder. The International Journal of Engineering and Science (IJES) 2(2), 1-8

22. Njoku, R. E, Okona, A. E., and Ikpakia, T. C., (2011) Effects Of Variation Of Particle Size And Weight Fraction On The Tensile Strength And Modulus Of Periwinkle Shell Reinforced Polyester Composite. Nigerian Journal of Technology l. 30(2).

23. Ihueze, C. C., Okafor, E. C., Ujam, A. J. (2012) Optimization of Tensile Strengths Response of Plantain Fibers Reinforced Polyester Composites (PFRP) Applying Taguchi Robust Design. Innovative System Design and Engineering, 3(7).

24. Acott, C. (1999) The diving Law-ers: A brief resume of their lives. South Pacific Underwater Medicine Society journal 29(1), 39-42.

25. IPC (1995) Test Methods Manual: Tensile Strength, Elongation and Modulus. Institute for Interconnecting and packaging electronic circuits, 2

26. Courtney, T.H. (1990) Mechanical Behavior of Materials. McGraw-Hill, New York.